Structures of solid hydrogen at 300K

Structures of solid hydrogen at 300K

Graeme J. Ackland[1] and John S. Loveday*

[1] *Centre for Science at Extreme Conditions and School of Physics and Astronomy, University of Edinburgh, Edinburgh, U.K.*

(Dated: March 6, 2020)

Abstract

We present simulated X-ray diffraction patterns (XRD) from molecular dynamics studies of phase transformations in hydrogen at room temperature. Phase changes can be easily identified in simulation, by directly imaging the atoms and measuring correlation functions. We show that the room temperature XRD patterns for hydrogen phases I, III, IV and V are very similar. The signature of the transformations in XRD are weak peaks and superlattice reflections denoting symmetry-breaking from the hcp Phase I, and a pronounced change in the c/a ratio. The XRD patterns implied by molecular dynamics calculations are very different from those arising from the static minimum enthalpy structures found by structure searching. Simulations also show that within Phase I, the molecules becomes increasingly confined to the basal plane and suggest the possibility of an unusual critical point terminating the Phase I-III boundary line. With these results, we propose a paradigm shift – that the predictions from DFT calculations should be seen as the most likely hypothesis. Specifically, we show that recent experimental results support the picture advanced by molecular dynamics simulations, and are inconsistent with the interpretation of an isostructural hcp transformation.

Solid hydrogen has proved to be one of the most challenging topics in high-pressure physics, both theoretically and experimentally. At room temperature, information about the crystal structure is available largely through indirect methods such as spectroscopy[1–8]. With the exception of two neutron diffraction studies[9,10] at $\sim$ 30GPa, structural studies are confined to X-ray studies[11–15] which are largely insensitive to molecular orientation. To exploit these studies fully, it is important to have models for the crystal structure. In recent years, *ab-initio* structure-search methods have been highly successful at determining the possible classical ground state structures[16–20]. These have shown a panoply of possible phases, typically with large unit cells and low symmetry, often very close in energy.

The calculations have an unquantifiable uncertainty associated with the choice of functional[21–24]. Furthermore, the effects of quantum nuclear-motion are significant, with zero-point energy being much larger than typical energy differences between structures. So despite all this work, no consensus has emerged for the crystal structure of any high pressure phase. Nevertheless, some patterns have emerged which suggest the calculated structures are consistent with the major experimental findings[25].

Since the discovery of a Raman-active phonon, Phase I of hydrogen has been accepted as a hexagonal close-packed (hcp) structure of rotating molecules. On cooling at pressure, a transformation occurs to a "broken symmetry" Phase II, characterized by a discontinuous change in H_2 vibron frequency and the appearance of several low-frequency modes. This transition occurs at temperatures and densities where quadrupole interactions become significant, and these are likely to be the driving force. The I-II transformation has no distinctive signature in X-ray diffraction[12], suggesting that it is an orientational ordering of the hydrogen molecules on the hcp lattice. Many of the most stable candidate structures from density functional theory (DFT) calculation are in this category.[16,26]

At higher pressures, above 160GPa at low-T, pronounced weakening in vibron frequency and further changes in the low frequency spectra heralds Phase III. It is debatable whether there is any signature of this phase in X-ray diffraction: at most it is a small distortion or modulation of the hcp structure. Perhaps the most distinctive signature of Phase III is the sudden appearance of a strong infrared signal, indicating that the structure has broken inversion symmetry. At still higher pressures, darkening of the samples suggests a reduced bandgap in a molecular phase[3,4,27], and reflectivity reveals a transition to a metallic phase[28,29], predicted by DFT to be initially molecular then a low-coordinated atomic solid.

Ultimately, hydrogen will metallize and the molecular bonds will break, though it is unclear whether these processes are simultaneous[30,31].

At room temperature, the Phase I transforms first to phase III at around 180GPa, then to a Phase IV at around 230GPa which has not been observed at low temperature. Phase IV is characterized by the appearance of a second, and possibly third, high frequency vibron[5,32–34]. Under further pressurization, the two vibrons remain and changes in the low frequency Raman spectra may indicate transformations to further phases IV' and V. It is assumed that metallization will occur, but this has not been observed at room temperature.

Our previous theoretical work has established that Phase II is a structure which minimizes the quadrupole energy[35], whereas phases I, III and IV are based on various stackings of triangular-lattice rotors (which we denote as B-layers) and orientationally ordered in-plane molecules (G-layers of various types: see Figs.1, 2).

We have spent several years making comparisons between DFT data obtained with the CASTEP code[36] and the spectroscopic data, using lattice dynamics and molecular dynamics, including path integral methods[25,37–43]. We have used different exchange-correlation functionals and different treatments of anharmonicity, and our conclusion is that these methods are not sufficiently accurate to obtain quantitative agreement for transition pressures or vibrational frequencies[22,39]. Nevertheless, in this paper we will present some predictions about crystal structures which are experimentally measurable.

A. ab initio molecular dynamics

Structure search algorithms work well for low temperature phases with harmonic phonons[16,20,44], but even at room temperature hydrogen is far from harmonic. Ab initio molecular dynamics (AIMD) is able to probe this region. Limitations on timescales and system sizes mean that accurate free energy calculations are impossible, however AIMD can reveal symmetry and structure of *candidate* phases.

Most previous AIMD was done with the PBE functional[45]. However, it is now becoming obvious that this *de facto* standard functional has a specific failing: it overstabilizes metallic structures relative to molecular ones. This can be traced to a design feature - PBE does not reproduce the energy in the limit of large $\nabla \ln(\rho)$. This does not usually cause problems: when studying metallic phases, the high $\nabla \ln(\rho)$ regime is not sampled, and in comparing

between molecular phases the error cancels out. It is only in the specific case of a molecule-metal transition that it becomes critical. In this work we also use the BLYP functional[46,47] which, though simple, does capture the high $\nabla \ln(\rho)$ limit and gives a better description of H_2 molecular dissociation[22].

1. *Phases*

Experimentally, five numbered solid phases have been reported based on spectroscopy. In addition, two "primed" sub-phases have been identified, giving a sequence I-I'-III-IV-IV'-V. The broken-symmetry phase II and metallic phases have been observed only at at low temperatures.

Previous MD on phases of hydrogen at 300K suggests only Phase III involves harmonic (or even anharmonic) oscillations about well-defined atomic positions all other phases have molecular rotation, reorientation, and at higher pressures significant rebonding. Unfortunately, previous calculations were done in the NVT ensemble, so that the crystallographic measurable, the c/a ratio, has not previously been calculated. For close-packing of hard spheres, the c/a ratio is $\sqrt{8/3} = 1.633$. Cohesion in solid hydrogen arises primarily from van der Waals forces which drop off as $1/r^6$. The Lennard-Jones potential captures this behavior, and stabilizes the hcp structure with $c/a < 1.633$, c/a is below ideal for almost all stable hcp materials[48], as we will find again here.

B. AIMD runs

We ran a large number of molecular dynamics calculations to evaluate the various structures. The same sequence of phases are observed independent of exchange-correlation functional. Compared with PBE, the BLYP functional gives systematically higher DFT pressures at a given density (Fig.4). It also makes better defined hydrogen molecules with higher vibrational frequencies.

Calculations were initiated from different candidate structures identified from previous *Ab-Initio* Random Structure Search, (AIRSS) calculations for phase II, III and IV candidates[16,17]. None of those low-symmetry structures remained stable at 300K, all transformed to higher symmetry structures. Nevertheless, based on average molecular positions

some distinct structures were observed which can be assigned to non-metallic phases I, III, IV, V plus a molecular metallic phase $Cmca$ and atomic metal $I4amd$.

1. *Finite Size Effects*

The large unit cells of phases III, IV and V mean that simulations are extremely sensitive to finite size effects. Only phases compatible with the supercell can be observed. e.g. the $BG'BG''$ phase IV candidate is hexagonal a four layer repeat with six atoms per layer - self evidently, only supercells with multiples of 24 atoms can find this structure, while the $BG'_xBG'_yBG'_z$ candidate requires a multiple of six hexagonal layers.

Furthermore, there is a probability of finding a layer with incorrect stacking. This is of order $\exp(-N\Delta F/kT)$, where ΔF is the excess free energy per atom in the mis-stacked layer and N the number of atoms per layer. This probability goes to zero at large N - *mis-stackings never occur in thermodynamic equilibrium.* However, in finite systems mis-stackings happen: with 12 atoms per layer, even fluctuations between B and G occur. We found that with less than 54 atoms *per layer* spurious fluctuations between types of G layer at the size of the system do still occur, which gives an incorrect mean-squared displacement which can be mistaken for diffusion.

For a simulation to even have the *possibility* of correctly distinguishing Phase IV, it should accommodate both $BG'BG''$ and $BG'_xBG'_yBG'_z$ candidates, and have layers containing a multiple of 6 atoms. To also prevent spurious fluctuations required a minimum of 648 atoms (i.e. 54 atoms per layer). This cell size was used in the region of the phase transition.

Finite size effects are generally regarded as a problem, but if properly understood they can be turned to advantage. Specifically, by adjusting the cell size to be incompatible with the stable phase, we can probe metastable phases. This enables us to predict experimental signatures for all candidate phases, and thus determine whether they could be distinguished by diffraction or spectroscopy.

All the cells considered can transform into Phase I, the simple hcp rotor phase. To identify the high pressure phases, we monitor three order parameters, the density, the c/a ratio and the angle between the molecules and the c-axis. We also use the VMD package to visualise the orderings. Qualitative results are similar for BLYP and PBE, with pressures calculated by PBE being systematically lower than those from BLYP.

At the lowest pressures Fig.3 shows that c/a in phase I tends from below to the ideal ratio, but becomes smaller under pressure. To understand why this might be, we examined the angle θ between the molecular axis and the c-axis (Fig.5). For a free rotor, $< \cos\theta >= 0.5$. This is the case at low pressure, but even within Phase I, as the pressure increases, the molecule increasingly rotates in the plane. This reduction of c/a has been observed by X-ray diffraction[12,13,15], and can now confidently be ascribed to the molecule changing from spherical to toroidal. The torus is still compatible with the $P6_3/mmc$, so this symmetry breaking of the molecule does not require a structural phase transition.

This change from spherical to torus rotation is not observed in NVT ensemble simulations with ideal c/a, emphasizing the importance of choice of ensemble.

At higher pressures there is a transformation to Phase III. Structure searching has revealed a number of candidate structures which were initially described by reference to the nuclear positions as different stackings of "distorted Graphite-like layers". However, considering the molecular (rather than atomic) positions reveals that those candidates were just an hcp lattice with the minimum of broken symmetry required for molecular orientation (Fig.1(a). AIMD shows a similar orientational ordering (see Fig.1b).

In figure 1 we show a schematic of how a layer in Phase III relates to Phase I. The large circles represent molecular locations on a perfect close packed plane. We observe that the molecules in Phase I come to lie in the plane at high pressure. Now, assume that each in-plane molecule points towards a gap between neighbour and is not aligned with its neighbours. These two rules are sufficient to uniquely define all the molecule orientations, as shown by the arrows. Figure 1 also shows a picosecond time-average from 648-atom BLYP simulation at 180GPa, assigned Phase III. Although the non-centrosymmetric motif is clear, there are frequent local rotations and reorientations.

This ordering leads to a 3-molecule repeat in the close-packed plane, and spontaneously breaks inversion symmetry. This broken symmetry means that the molecule moves off the hcp site and acquires a dipole moment which responsible for the strong IR signal of Phase III. The movement off-site might be detectable by X-ray scattering from superlattice reflections, but only induces a small change in relative intensity of the three main peaks compared with hcp.

Furthermore, there are two non-equivalent sites for the next layer (2/3rds unmarked, 1/3rd red circles). The lowest energy structures identified by ab initio structure search for

Phase III, $C2/c-24$ and $P6_122$, involve a 4 and 6 layer repeat of this 2D-layer.

To understand the highest pressure phases IV-V, Fig.2 relates the observed structures to the simple MgB_2 structure with a hydrogen molecule on the Mg site (a triangular "B" layer) and hydrogen atoms on the boron sites (a graphitic layer "G"). This structure has alternating layers, so the c-glide symmetry is broken and the space group becomes $P6/mmm$. In the molecular dynamics, this MgB_2 structure is recognised *on average* at very high pressures. However it is energetically highly unstable to formation of molecules: the trajectories cannot be described in terms of harmonic oscillations.

The structures observed for phases IV, IV' and V are described in terms of symmetry-breaking from MgB_2 so as to form molecules in the G-layers. There are multiple ways of doing this (Figure 2). The molecules in these layers tend to remain in plane, meaning that the equivalent c/a ratio falls below that of hcp.

Determination of the high temperature structures was done by painstaking layer-by layer visual analysis using vmd. In addition to snapshots or movies, two analyses proved extremely useful.

- Plots of time-averaged atomic positions. The B-layers image as a triangular lattice with two atoms coincident at each lattice site. The G'' layers image as a large triangular lattice with six atoms coincident at each site. The G' layers typically image as separate atoms, similar to a snapshot, although after many picoseconds the pattern is destroyed by diffusion within this layer.

- Dot-plots for all atoms, at all times. The B-layer molecules image as spheres or small donuts, the G'' layers image as triple-arcs or large donuts, with some evidence of six- and three-fold rotational symmetry, the G' layers image as separate atoms.

We carried out limited path integral molecular dynamics, which show relatively little qualitative change from the classical picture, the main effect being a wider variation in molecular length due to zero-point energy. There is some small effect on the phase boundaries and c/a ratio.

2. Simulated XRD Crystallography

We have calculated the powder diffraction pattern from the positions of the atoms from a sample of MD runs in phases I, III, IV and V. This was done by combining the positions from the final 2ps of the MD trajectory and treating the supercell as a single cell with P1 symmetry. The resulting assemblage of approximately 50000 atomic positions thus models not only the average positions of the atoms within the structure but also the atomic displacements, including anisotropy and anharmonicity, about these average positions. The calculations were done using the GSAS-II program[49] and assumed a standard hydrogen form factor and an X-ray wavelength of 0.7 Å.

Figure 6 shows that at 140GPa, the XRD patterns for two lowest energy candidate structures for Phase II $P6_3/m$ and $Pca2_1$ are similar, the distinguishing feature being a small peak splitting in $Pca2_1$. Simulated XRD gives 3 significant diffraction peaks, which could be misinterpreted as (100) (002) and (101) from an hcp structure if the weaker peaks are ignored. MD simulations at 300K, started in either $P6_3/m$ or $Pca2_1$ transform to a hindered-rotor hcp Phase I.

Phase III is stable at 190GPa, and Fig.7 shows that again the two zero-temperature candidate structures $P6_122$ and $B2/n$ (sometimes called by its alternative setting $C2/c$) have similar 2-peak patterns, being distinguished only by weak reflections. In the MD, the two-peak pattern persists, but unusually as the temperature increases, a third small peak grows in prominence, while other small peaks vanish. Visualization of our MD (Fig.1) makes it clear that we have Phase III, but the simulated pattern differs from the diffraction pattern for hcp only in some weak peak. Our strongest superlattice peak is at $(\sqrt{\frac{1}{3}}, 0, \frac{1}{3})$, outside the reported range of experimental XRD[15].

On simulated isobaric heating above 300K, the XRD pattern transforms continuously to be characteristic of phase I, consistent with the gradual loss of orientational order. This suggests a second order transition, or maybe even a I-III boundary line terminating in a critical point. Unusually, the (100) peak becomes more pronounced with increasing temperature, implying that the charge density is better localised in the plane. This occurs because at low T, the molecules are preferentially out of the (001) plane, while at high-T the rotation means that this preference weakens.

There are several candidates for Phase IV: Fig.8 shows clear discrepancy between the

peaks identified experimentally by Ji et al, and the P63/mmc DFT structure proposed in that work. From our MD we identified two possible structures (BG'BG" and $BG_xBG_yBG_z$). These two candidates give similar patterns with a very close doublet and a third peak at larger d-spacing. Ignoring the small peaks, would be possible to index these peaks to hcp, with a small $c/a = 1.52$ ratio. Structure search for these pressures gave Cmca and Ibam as energy-favoured candidates: Fig.8 shows both variants of Cmca are inconsistent with the data; Ibam, which is stable in MD above 450GPa[37,50], could be easily distinguished from hcp, and is conclusively excluded below 250GPa by the XRD data[15].

Ji *et al*[15] have observed the characteristic drop in the c/a ratio associated with the phase I-III-IV transitions above, and attribute it to an isostructural transition within the hcp (P63/mmc) space group. This would be a unique example of an isostructural electronic transition between two non-metallic phases. We have recalculated this P63/mmc structure using BLYP and PBE, reproduced the band structure and find it to be energetically unstable at all pressures. Furthermore, the c/a ratio for this structure (blue squares, Fig.3) *increases* with pressure, in conflict with their own XRD evidence. This result is not presented by Ji *et al*, and the calculated energetic instability of P63/mmc is further evidence *against* the existence of any such isostructural transition. At all pressures, this P63/mmc is unstable in AIMD to phase I, III or IV.

The original 1935 prediction of metallic hydrogen by Wigner and Huntingdon[51] is based on free electron theory, and analysis of metallic hydrogen is still based on this premise[52]. Since hydrogen has no core electrons, a free-electron phase of solid hydrogen would have a featureless X-ray diffraction pattern. However, calculations using DFT show that in the atomic phase,I4amd, the electrons are still well localized, and X-ray diffraction from metallic hydrogen will be nearly as strong as from molecular phases[53].

C. Discussion and Conclusions

We have carried out extensive molecular dynamics simulations of high pressure hydrogen at room temperature using two different exchange correlation functionals. The functionals give the same sequence of phases, but with a difference of 20-30GPa in pressure. The sequence of phases, I-III-IV-V is in accordance with experiment, with the calculated transition pressures being lower. Molecular rotation (or disorder) increases the symmetry so that the

calculated diffraction pattern for Phases III and IV is much more similar to Phase I than to their zero-temperature relaxed structures.

Under pressure the free rotors of Phase I become more and more inhibited, with the molecules preferentially rotating in-plane. This loss of sphericity causes a drop in the c/a ratio away from ideal. In phase III, the rotation stops and the molecules lie in plane, however the diffraction pattern structure is still close to hcp with a still-lower c/a ratio. A pronounced drop in the c/a ratio and change in its pressure-slope accompanies the transformation.

We have simulated the XRD patterns from our MD, and find that all structures produce three strong peaks which could be indexed by hcp. The only strong signatures of the phase transformation in XRD are a steep drop in the c/a ratio with pressure and some superlattice reflections. Ji et al identify only three reflections indexed as hcp, and despite multiple spots their patterns cannot produce reliable intensities, so the structural information comes only from the c/a ratio.

Fig.9 shows the striking disagreement between the XRD in Ji's paper (c/a reduces with pressure), and their own calculated structure (c/a increases with pressure, with no discontinuity at the calculated isostructural transition). The most energetically stable hexagonal structure known from structure search ($P6_122$) is in better agreement, but does not show any isostructural transition. Only the MD simulation correctly reproduces the XRD behaviour, with a steadily decreasing c/a ratio that drops sharply at the phase transition, albeit at a lower pressure. The room temperature, high pressure phases of hydrogen can therefore confidently be ascribed to hexagonal structures with inhibited rotors, and unit-cell tripling, up to at least 250GPa.

Fig.9 shows an offset of about 50GPa between the calculated and measured transition pressure. This is similar to the systematic errors due to functional (see Fig.3), the omission of nuclear quantum effects and the conversion from diamond edge frequency to GPa[39].

In conclusion, we have shown that AIMD simulations predict a series of phase transformations corresponding to hydrogen Phases I, III and IV, and that those transformations are consistent with the recent XRD experiment by Ji *et al.* The MD structures all have higher symmetry than anything found by AIRSS. Phases III and IV are hexagonal, but have lower symmetry, and much larger unit cells, than hcp. We advocate that candidate structures from AIMD should be regarded as a null hypothesis for interpreting experimental data.

Acknowledgments

The authors acknowledge the support of the European Research Council Grant Hecate Reference No. 695527 and UCKP collaboration EPSRC grant PO22561.

---

* g.j.ackland@ed.ac.uk

[1] A. F. Goncharov, R. J. Hemley, H.-K. Mao, and J. Shu, Phys.Rev.Letters **80**, 101 (1998).

[2] A. F. Goncharov, E. Gregoryanz, R. J. Hemley, and H.-K. Mao, Proceedings of the National Academy of Sciences **98**, 14234 (2001).

[3] P. Loubeyre, F. Occelli, and R. LeToullec, Nature **416**, 613 (2002).

[4] P. Dalladay-Simpson, R. T. Howie, and E. Gregoryanz, Nature **529**, 63 (2016).

[5] R. T. Howie, C. L. Guillaume, T. Scheler, A. F. Goncharov, and E. Gregoryanz, Phys. Rev. Letters **108**, 125501 (2012).

[6] C. S. Zha, Z. Liu, and R. J. Hemley, Phys. Rev. Letters **108**, 146402 (2012).

[7] R. T. Howie, P. Dalladay-Simpson, and E. Gregoryanz, Nature materials **14**, 495 (2015).

[8] E. Gregoryanz, A. F. Goncharov, K. Matsuishi, H.-K. Mao, and R. J. Hemley, Phys.Rev.Letters **90**, 175701 (2003).

[9] V. Glazkov, S. Besedin, I. Goncharenko, A. Irodova, I. Makarenko, V. Somenkov, S. Stishov, and S. Shilshtein, JETP Letters **47**, 763 (1988), ISSN 0021-3640.

[10] I. Goncharenko and P. Loubeyre, Nature **435**, 1206 (2005).

[11] R. Hemley, H. Mao, L. Finger, A. Jephcoat, R. Hazen, and C. Zha, Physical Review B **42**, 6458 (1990).

[12] P. Loubeyre, R. LeToullec, D. Hausermann, M. Hanfland, R. Hemley, H. Mao, and L. Finger, Nature **383**, 702 (1996).

[13] Y. Akahama, M. Nishimura, H. Kawamura, N. Hirao, Y. Ohishi, and K. Takemura, Phys. Rev. B **82**, 060101 (2010).

[14] Y. Akahama, H. Kawamura, N. Hirao, Y. Ohishi, and K. Takemura, in *Journal of Physics: Conference Series* (IOP Publishing, 2010), vol. 215, p. 012056.

[15] C. Ji, B. Li, W. Liu, J. S. Smith, A. Majumdar, W. Luo, R. Ahuja, J. Shu, J. Wang, S. Sinogeikin, et al., Nature **573**, 558 (2019).

[16] C. J. Pickard and R. J. Needs, Nature Physics **3**, 473 (2007).

[17] C. J. Pickard and R. J. Needs, Physica Status Solidi (b) **246**, 536 (2009).

[18] C. J. Pickard, M. Martinez-Canales, and R. J. Needs, Phys. Rev. B **85**, 214114 (2012).

[19] X.-Z. Li, B. Walker, M. I. Probert, C. J. Pickard, R. J. Needs, and A. Michaelides, Journal of Physics: Condensed Matter **25**, 085402 (2013).

[20] B. Monserrat, R. J. Needs, E. Gregoryanz, and C. J. Pickard, Physical Review B **94**, 134101 (2016).

[21] S. Azadi and W. M. C. Foulkes, Phys. Rev. B **88**, 014115 (2013).

[22] R. C. Clay III, J. Mcminis, J. M. McMahon, C. Pierleoni, D. M. Ceperley, and M. A. Morales, Phys. Rev. B **89**, 184106 (2014).

[23] N. D. Drummond, B. Monserrat, J. H. Lloyd-Williams, P. L. Ríos, C. J. Pickard, and R. J. Needs, Nature communications **6** (2015).

[24] S. Azadi and G. J. Ackland, Physical Chemistry Chemical Physics **19**, 21829 (2017).

[25] I. B. Magdău, M. Marques, B. Borgulya, and G. J. Ackland, Phys.Rev.B **95**, 094107 (2017).

[26] H. Y. Geng, H. X. Song, J. Li, and Q. Wu, Journal of Applied Physics **111**, 063510 (2012).

[27] M. Eremets and I. Troyan, Nature materials **10**, 927 (2011).

[28] R. P. Dias and I. F. Silvera, Science **355**, 715 (2017).

[29] P. Loubeyre, F. Occelli, and P. Dumas, Nature **577**, 631 (2020).

[30] B. Holst, R. Redmer, and M. P. Desjarlais, Physical Review B **77**, 184201 (2008).

[31] W. Lorenzen, B. Holst, and R. Redmer, Phys. Rev. B **82**, 195107 (2010).

[32] R. T. Howie, T. Scheler, C. L. Guillaume, and E. Gregoryanz, Phys. Rev. B **86**, 214104 (2012).

[33] C. S. Zha, Z. Liu, M. Ahart, R. Boehler, and R. J. Hemley, Phys.Rev.Letters **110**, 217402 (2013).

[34] P. Loubeyre, F. Occelli, and P. Dumas, Phys. Rev. B **87**, 134101 (2013).

[35] S. van de Bund and G. J. Ackland, Physical Review B **101**, 014103 (2020).

[36] S. J. Clark, M. D. Segall, C. J. Pickard, P. J. Hasnip, M. I. Probert, K. Refson, and M. C. Payne, Zeitschrift für Kristallographie-Crystalline Materials **220**, 567 (2005).

[37] I. B. Magdău and G. J. Ackland, Phys. Rev. B **87**, 174110 (2013).

[38] I. Magdău and G. J. Ackland, **500**, 032012 (2014).

[39] G. J. Ackland and I. B. Magdău, Cogent Physics **2**, 1049477 (2015).

[40] R. T. Howie, I. B. Magdău, A. F. Goncharov, G. J. Ackland, and E. Gregoryanz, Phys. Rev.

Letters **113**, 175501 (2014).

[41] G. J. Ackland and I. B. Magdău, High Pressure Research **34**, 198 (2014).

[42] I. B. Magdău, F. Balm, and G. J. Ackland, Journal of Physics: Conference Series **950**, 042059 (2017).

[43] I. B. Magdău and G. J. Ackland, Phys. Rev. Lett. **118**, 145701 (2017).

[44] M. Martinez-Canales, A. R. Oganov, Y. Ma, Y. Yan, A. O. Lyakhov, and A. Bergara, Physical review letters **102**, 087005 (2009).

[45] J. P. Perdew, K. Burke, and M. Ernzerhof, Phys.Rev.Letters **77**, 3865 (1996).

[46] C. Lee, W. Yang, and R. G. Parr, Physical review B **37**, 785 (1988).

[47] A. D. Becke, Physical review A **38**, 3098 (1988).

[48] C. H. Loach and G. J. Ackland, Physical review letters **119**, 205701 (2017).

[49] B. H. Toby and R. B. von Dreele, Journal of Applied Crystallography **46**, 544 (2013).

[50] I. B. Magdău, B. Tyson, B. Borgulya, and G. J. Ackland, writing (2016).

[51] E. Wigner and H. Huntington, J. Chem. Physics **3**, 764 (1935).

[52] R. P. Dias, O. Noked, and I. F. Silvera, Phys.Rev.Letters **116**, 145501 (2016).

[53] Ingo Loa, private communication

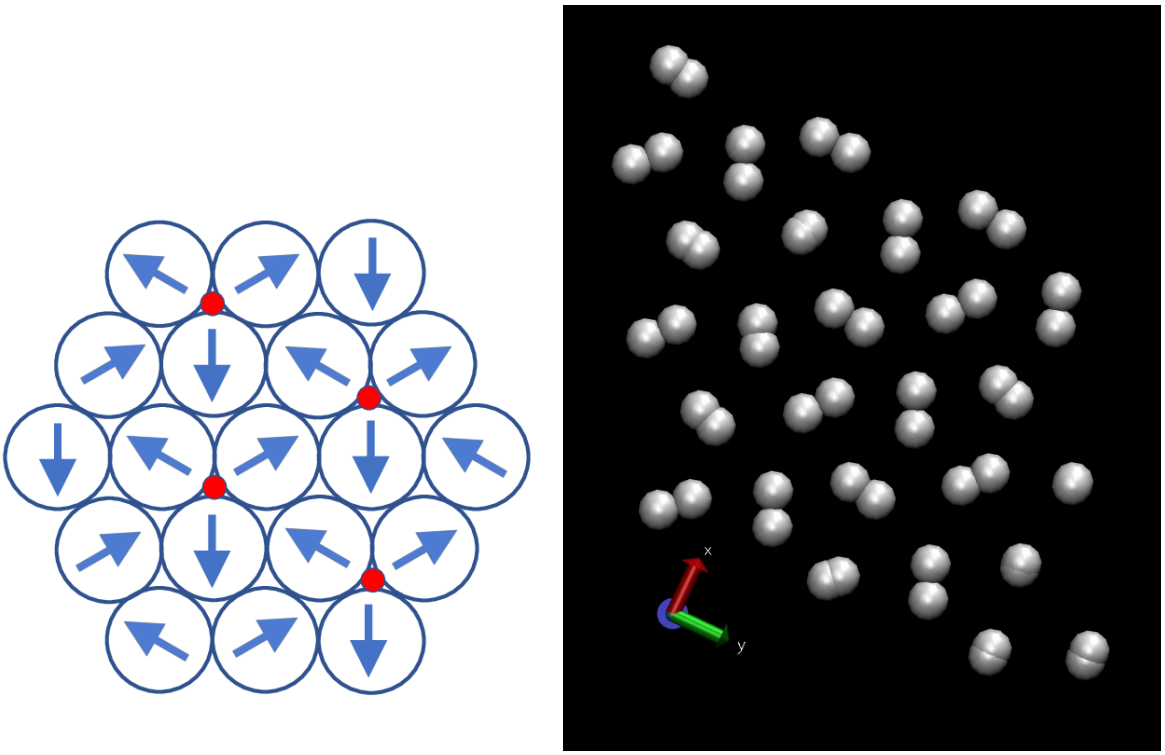

FIG. 1: Single G layer, All structures comprising stacking of these layers are labelled "Phase III'. (left) schematic: red dots show position of the 3-fold rotation axis. Blue arrows represent molecular axis. The orientational transformation breaks the symmetry and induces a dipole, as indicated by the direction the arrow. (right) time-averaged positions of atoms aver 1ps from one layer in the 180GPa simulation using BLYP. All molecules are in-plane, apparently-short bonds occur when the molecule has rotated through 180 degrees at some stage. Notice how molecular centres are slightly displaced from hcp sites.

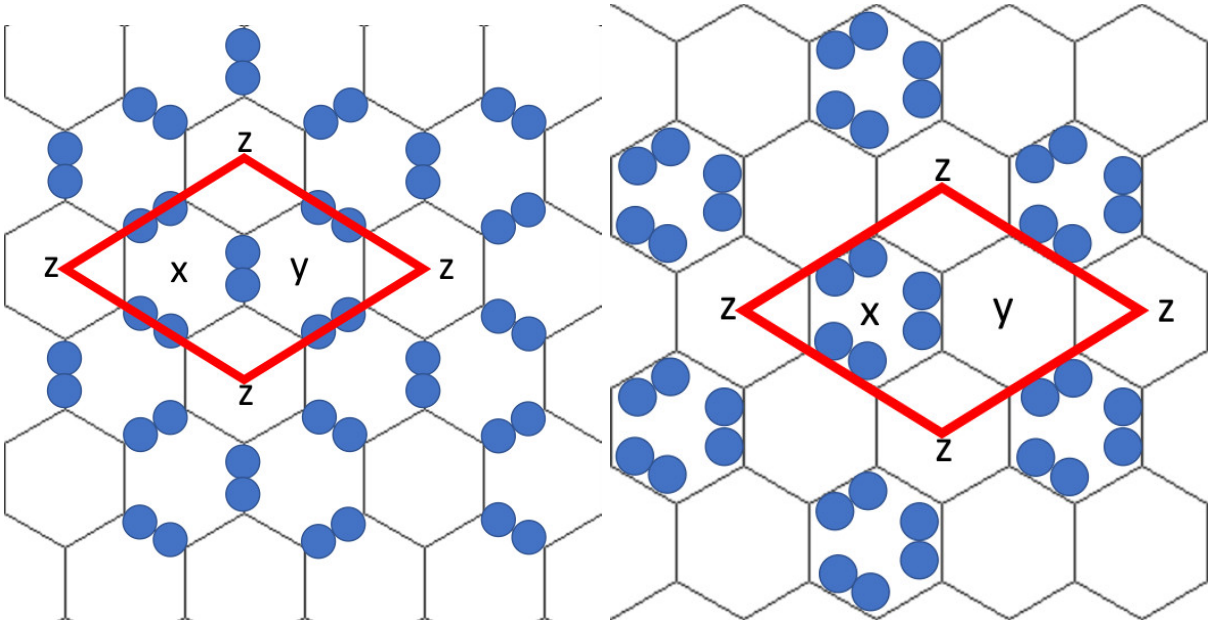

FIG. 2: Schematic of typical in-plane atomic positions in the so-called "graphitic" (G) layers of Phase IV. The red diamond shows a and b vectors for single unit cell. Each unit cell has two equivalent and one non-equivalent hexagon: x, y and z are used to label the layer stacking of the non-equivalent site. In this notation (a) G'_z, (b) G''_x. The molecular "B"-layers are like Phase-I and are not shown, they simply comprise a molecule at the center of each hexagon, again six atoms per layer. In static relaxation these B-molecules have well defined orientation (e.g. the Pbcn structure), but at room temperature they are disordered and re-orient on a 100fs timescale. Due to constraints from periodic boundary conditions, in MD simulation a two-layer cell in Phase IV PT conditions adopts BG'_z stacking, four layers $BG'_zBG''_z$, six layers $BG'_xBG'_yBG'_z$, eight layers $BG'_zBG''_zBG'_zBG''_z$ twelve layers $BG'_xBG'_yBG'_zBG'_xBG'_yBG'_z$.

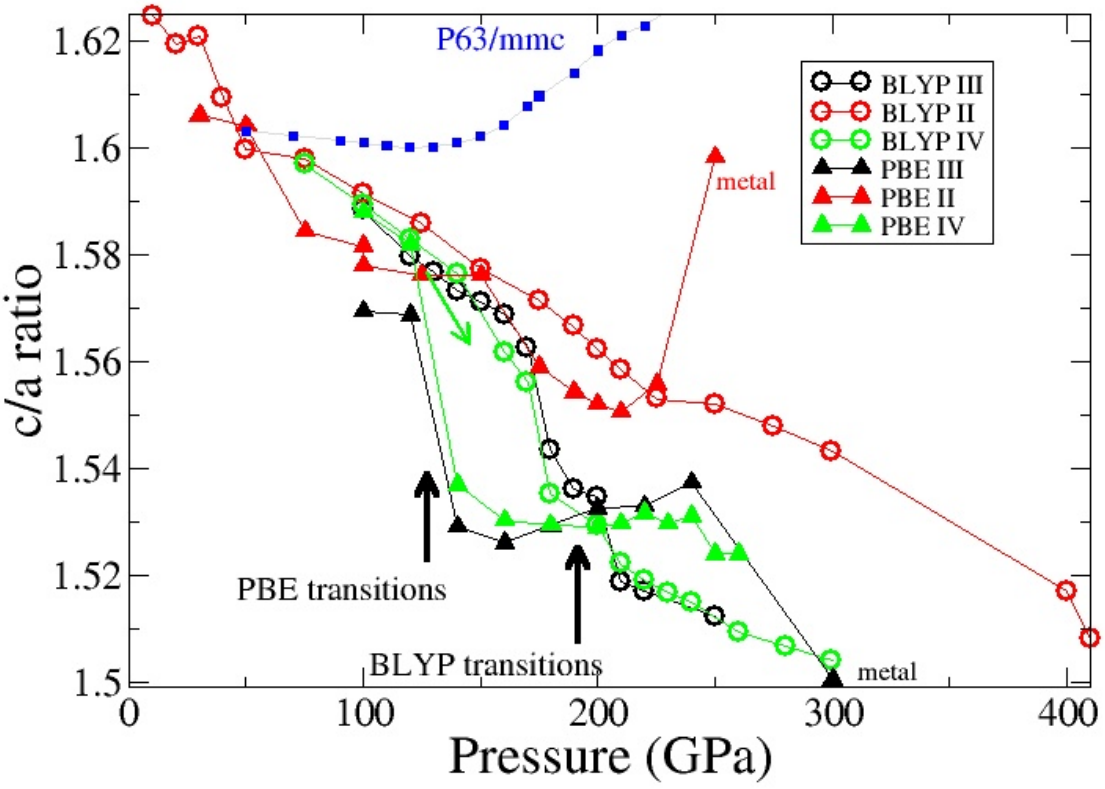

FIG. 3: Plot of c/a ratio for simulations in various cells. Arrows show sharp change in c/a with transition to phase IV, and more gradual change approaching phase III. Note the significant functional dependence in the calculated transition pressure. The very high pressure metallic Cmca structures are twinned, so the change in "c/a ratio" for the simulation cell signifies the transition, but is not the c/a ratio of Cmca. d-spacings can be calculated from the c/a ratio and the volume per molecule ($\sqrt{3}ca^2/4$): The observed d-spacings are: $(100) = \sqrt{3}a/2$, $(101) = \sqrt{(3a^2/4 + c^2)}$ and $(002) = c/2$.

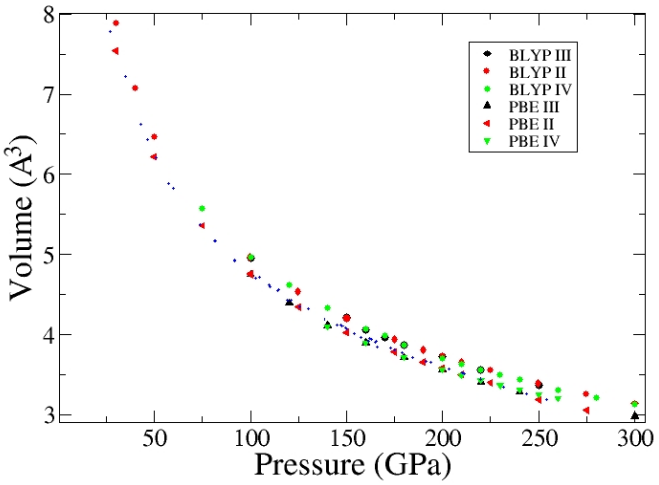

FIG. 4: Equation of state (volume per atom at 300K) for all structures with BLYP (circles) and PBE (triangles) showing that functional effects are much larger than structural differences, and the uncertainty due to functional is about 20GPa. Small blue dots are XRD data[15].

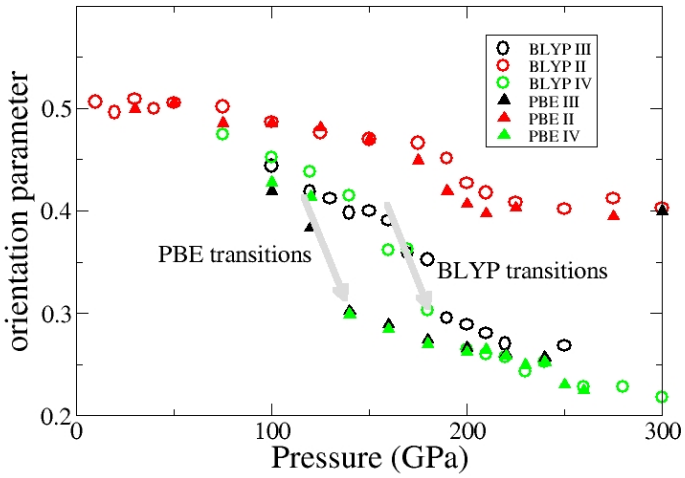

FIG. 5: Variation of orientation order parameter $< \cos\theta >$ with pressure at 300K. Incompatibility with boundary conditions means that the transition to phase III or IV is suppressed in the red "Phase II" simulations which started in $P6_3/m$ symmetry. Transitions were also identified from visualization of trajectories.

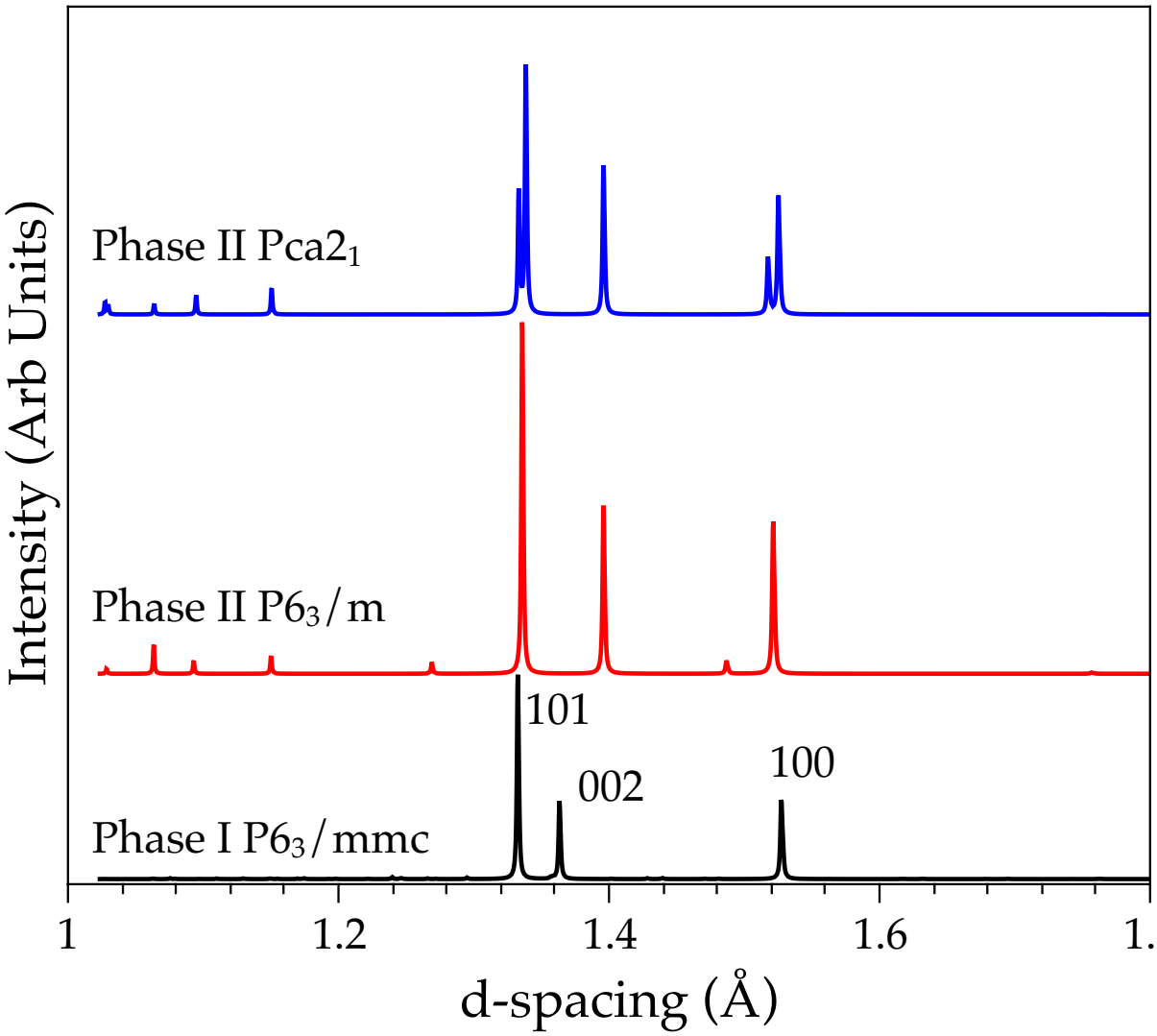

FIG. 6: Simulated X-ray diffraction patterns for Hydrogen Phase II at 140GPa. P6$_3/m$ and P$ca2_1$ are the zero-temperature ground states proposed by structure search. Black line is MD starting from P6$_3/m$ at 300K temperature: MD starting from P$ca2_1$ or P6$_3/mmc$ are indistinguishable - all are hcp Phase I with hkl indexing as shown.

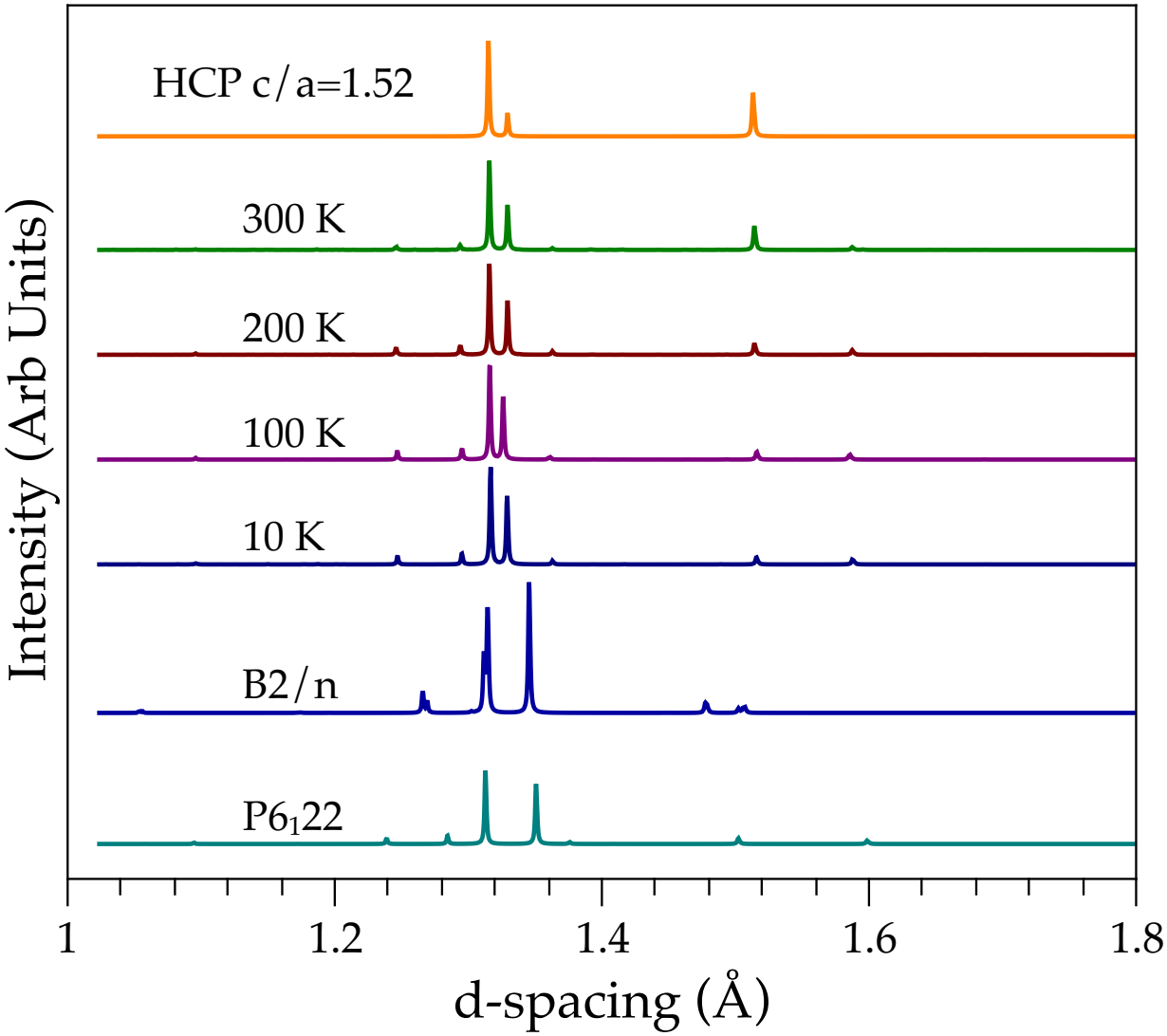

FIG. 7: Simulated X-ray diffraction patterns for Hydrogen Phase III at 190GPa calculated using BLYP. B2/n and P6$_1$22 are the zero-temperature ground states proposed by two structure-search calculations[16,20]. MD lines are labelled by temperature and are averaged over 2ps starting from P6$_1$22 at various temperatures. The pattern for *hcp*, the proposed solution for Ji *et al*'s[15] room temperature XRD patterns, is shown for comparison. In addition to the hcp-like peaks shown, the MD also predicts a superlattice reflection at a larger d-spacing around 2.65Å, with $hkl = (\sqrt{\frac{1}{3}}, 0, \frac{1}{3})$. Ji *et al* do not index such small-angle data.

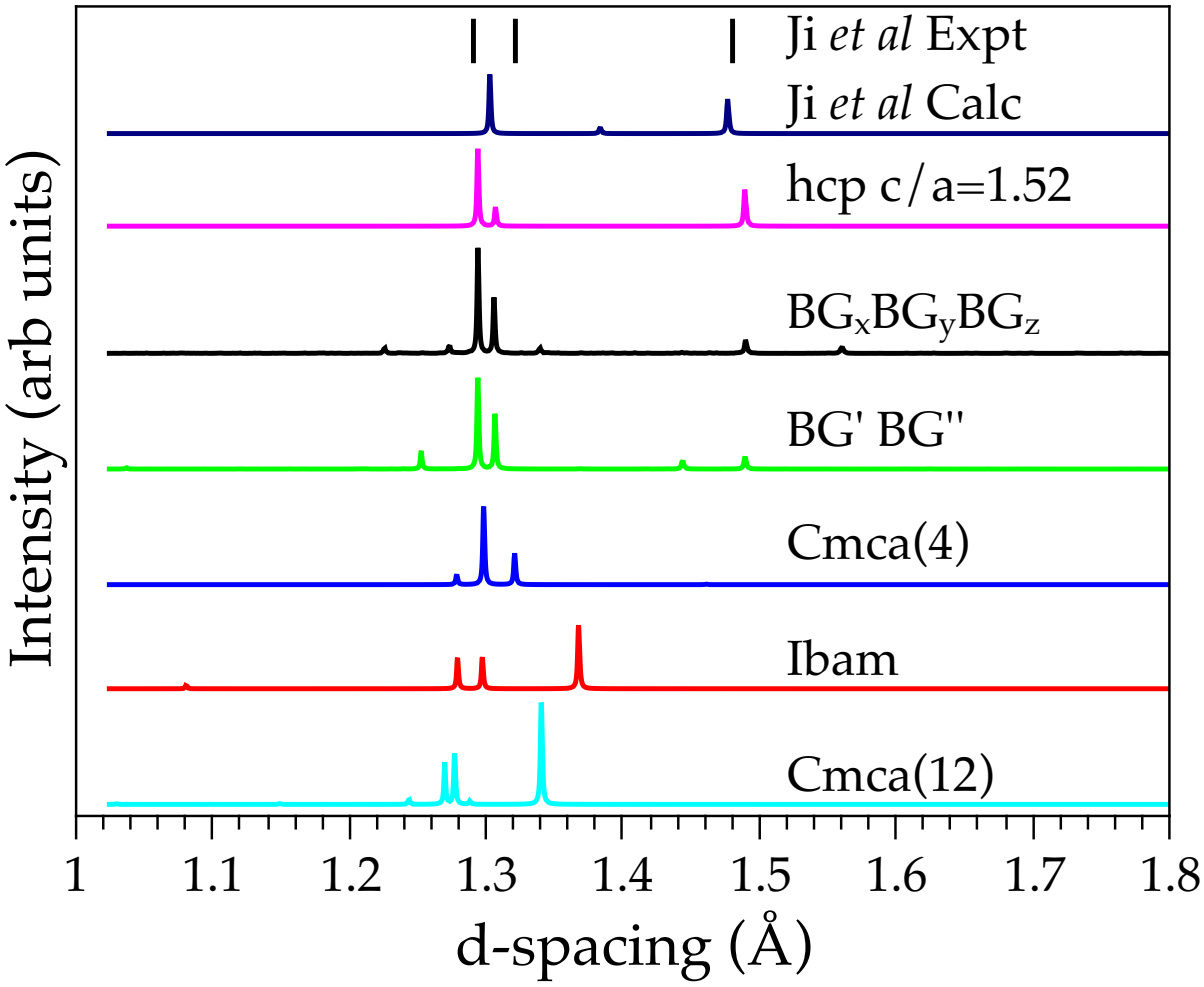

FIG. 8: **Simulated X-ray diffraction patterns for Hydrogen Phase IV at DFT-Pressure of 220GPa.** Tick marks show XRD data from Ji *et al* at equivalent density assigned to $(100)_{hcp}$ $(002)_{hcp}$ and $(101)_{hcp}$, alongside the pattern from the $P6_3/mmc$ structure calculated in Ji *et al*, and simple hcp. Our MD for the two different hexagonal candidates (Fig. 2), is averaged over 2ps at 300K starting from $P6_122$ ($BG_xBG_yBG_z$) and starting from P*bcn* ($BG'BG$"). Cmca(4) Cmca(12) and Ibam are the zero-temperature ground states found by structure search[16]

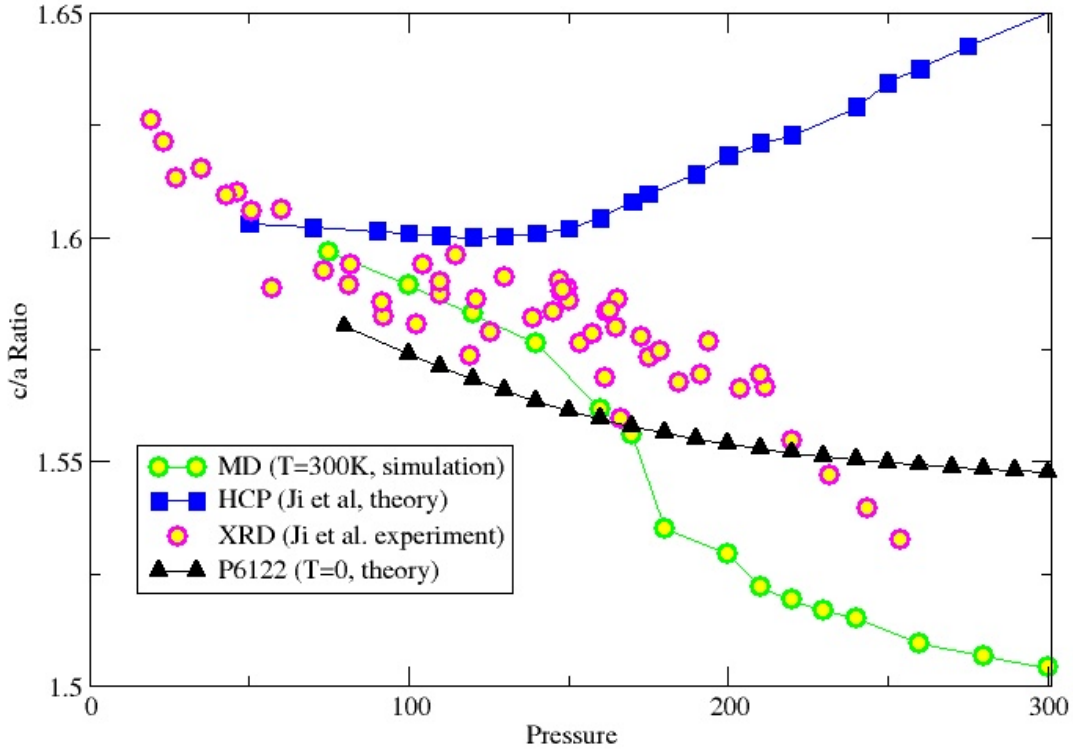

FIG. 9: Comparison of hexagonal c/a ratio for experimental XRD[15] (magenta) with DFT: Isostructural hcp $P6_3/mmc$ (blue squares), structure search enthalpy minimum $P6_122$ (black triangles) and MD (green circles). All DFT calculations used BLYP functional, and previously-reported results[15,20] were replicated in this study.